

# RESEARCHES ON HEAT DISSIPATION CHARACTERISTICS OF INTEGRATED CONTROLLER IN-WHEEL MOTOR

Jie Jiao<sup>1</sup>, Youtong Zhang<sup>1\*</sup>, Liqing Sun<sup>1</sup>, Tao Li<sup>1</sup>

<sup>1</sup> School of Mechanical Engineering, Beijing Institute of Technology, Beijing 100081, China

## ABSTRACT

This paper presents the heat dissipation problem of an integrated controller in-wheel motor. The temperature field of the in-wheel motor is calculated based on the finite element method. The temperature rise law of the stator winding and IGBT is analyzed, and a cooling channel structure which can simultaneously cool the in-wheel motor and the control system is proposed. The experimental results show that the cooling effect is optimal when the flow rate of the cooling water is 4 L/min, the winding temperature is reduced by 31 °C, and the IGBT temperature is reduced by 49.65 °C. The simulation accuracy error is less than 6.3 %, and the heat dissipation model has a high precision.

**Keywords:** integrated controller in-wheel motor, heat loss model, combined water channel, temperature field

## 1. INTRODUCTION

The in-wheel motor drive technology is considered to be the most ideal driving form for the future of the car. Its simple structure and high power density make it a great development space in the electric vehicle field. However, due to the limitation of the working environment and installation space, the motor heat dissipation conditions are extremely harsh. When the heat is severe, it will have many negative effects on the performance of the motor, such as the motor insulation performance caused by high temperature, reduced life, permanent magnet demagnetization, accelerated winding aging, etc. Therefore, it is very important to research on motor cooling technology which has theoretical and practical significance. A. Nollau et al. [2] proposed a cooling method for a motor on a hybrid or pure electric vehicle. The method uses a vortex tube to generate -40 °C cooling air to cool the motor, but has not

been experimentally verified, although the cost of the vortex tube is very low, the feasibility of this method still needs to be considered. F. Luise et al. [3] developed a high-performance 640 kW, 10000 r/min high-speed permanent magnet motor prototype. The cooling system uses a combination of air-cooling and water-cooling, including a cylindrical aluminum water jacket surrounding the stator core and a forced axial air flow for the rotor to dissipate heat. Xiaoyi Li et al. [4] proposed a reciprocal axial two-channel liquid-cooling structure, which divides the original single-channel into two, and sets two pairs of inlet and outlet to form two reciprocal channels, which can avoid local hot spots in the motor. The maximum temperature rise is reduced, but the structural complexity is brought about.

In this paper, in order to reduce the temperature of the integrated controller in-wheel motor and improve its efficiency, a combined cooling channel is designed and the influence of the water channel on the heat dissipation characteristics of the motor is analyzed.

## 2. IN-WHEEL MOTOR THERMAL PROBLEM

Fig. 1 shows the model of the in-wheel motor. The experimental conditions are selected as low-speed and high-torque conditions. The speed is 400 r/min and the torque is 120 Nm, the output power is 5 kW. Table 1 shows the parameters of the in-wheel motor.

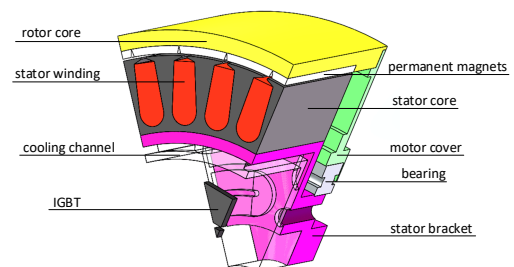


Fig. 1 In-wheel motor model

Table 1. Basic parameters of the in-wheel motor

Rated power /kW	Rated voltage /V	Rated speed /r·min <sup>-1</sup>	Rated frequency /Hz
10	190	1000	266

### 2.1 Heat loss model

Motor losses mainly consist of stator copper loss, stator core loss, rotor eddy current loss, mechanical loss and IGBT loss, which can be derived from equations (1) - (4):

$$P_{Cu} = 3I_{rms}^2 R_{dc} \quad (1)$$

$$P_{Fe} = V_{Fe} (K_h f B_m^\alpha + K_e f^2 B_m^2 + K_{exc} f^{1.5} B_m^{1.5}) \quad (2)$$

$$P_r = \int_z \left( \frac{J_z J_z^*}{\sigma_e} \right) ds \quad (3)$$

$$\begin{cases} P_f = k C_f \rho_0 \pi \omega_m^3 r^4 L \\ P_b = C_b D_m^3 \omega_m \end{cases} \quad (4)$$

where  $I_{rms}$  is the effective value of the phase current,  $R_{dc}$  is the single-phase winding DC resistance,  $V_{Fe}$  is the core volume,  $K_h$  and  $\alpha$  are hysteresis loss coefficients,  $K_e$  is the eddy current loss coefficient,  $K_{exc}$  is the additional loss coefficient,  $f$  is the magnetic field alternating frequency,  $B_m$  is the magnetic field amplitude,  $J_z$  is the permanent magnet z-direction current density,  $\sigma_e$  is the conductivity,  $k$  is the rotor surface roughness,  $C_f$  is the friction coefficient,  $\rho_0$  is the gas density,  $\omega_m$  is the rotor angular velocity,  $r$  is the rotor radius,  $L$  is the rotor length,  $C_b$  is the bearing coefficient which could be provided by the manufacturer,  $D_m$  is the bearing diameter.

Table 2 shows the calculated loss.

Table 2. In-wheel motor loss distribution

Loss /W	Stator copper loss	Stator core loss	Rotor eddy current loss
Value	10	63.2	37.4
Loss /W	Rotor core loss	Mechanical loss	IGBT loss
Value	90.6	3.63	707.3

### 2.2 Motor heat distribution

Based on the heat loss model, the temperature field analysis of the in-wheel motor is performed by COMSOL

Multiphysics. The temperature rise distribution of the stator winding and the IGBT is shown in Fig. 2 and Fig. 3. It can be seen that the average temperature of stator winding is around 69.27 °C, and the average temperature of IGBT is around 100.22 °C. The overall temperature rise of the motor is high, so it is necessary to design the cooling system of the motor.

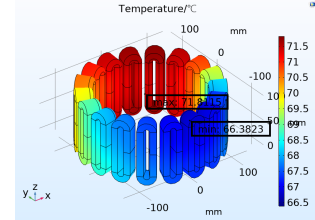


Fig. 2 No cooling winding temperature distribution

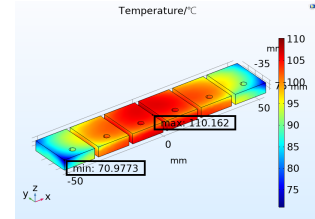


Fig. 3 No cooling IGBT temperature distribution

## 3. COOLING CHANNEL DESIGN AND SIMULATION

### 3.1 Cooling channel structure

Cooling channel usually comes in many different forms, but totally can be divided into two major categories, axial Z-shape and spiral shape. Because of the particularity of the outer rotor in-wheel motor and the integrated controller inside the motor, the cooling channel shown in Fig. 4 is designed in combination with the characteristics of the two channels.

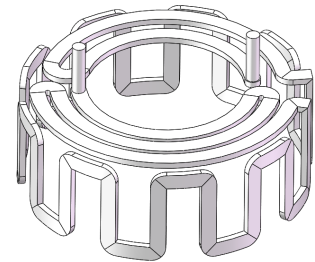


Fig. 4 Cooling channel model

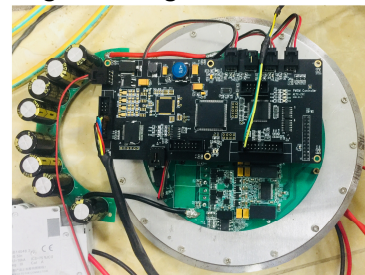


Fig. 5 External channel with control board

In order to facilitate the disassembly and assembly of the motor, the external water channel method is actually used to simulate the cooling effect inside the motor, which is convenient for the experiment. Fig. 5 shows the the external water channel with the control board.

### 3.2 Thermal model simulation

The following assumptions are invoked in the analysis.

1. The materials of all parts of the motor are isotropic.
2. Ignore the contact thermal resistance, that is, the contact surface between the solid and solid has the same temperature, such as between the stator core and the stator support, between the permanent magnet and the rotor core.
3. The cooling water can take away all the heat generated by the loss.
4. The air gap inside the motor and the gas at the end of the winding are regarded as isothermal bodies.
5. Ignore the effect of temperature on the properties of the part.
6. Ignore the phenomenon of heat radiation.

Fig. 6 shows the steady-state temperature rise distribution of the stator windings under different flow rates. It can be found that when the cooling flow is small, the winding exhibits a distinct phenomenon of cold and heat boundary. As the cooling flow increases, the overall temperature rise of the stator winding gradually becomes uniform. The cause of this phenomenon is due to the cooling channel as the axis. To the Z type, the cooling effect on the motor is gradually changed along the side. The cooling effect was considered to be good at 4 L/min, and the steady-state temperature at this time was 35.8 °C.

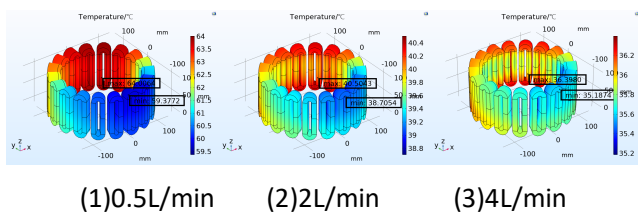


Fig. 6 Stator windings temperature rise distribution under different flow rates

Fig. 7 shows the steady-state temperature rise distribution of IGBTs at different flow rates. It can be seen that as the flow rate of the cooling water increases, the temperature of the IGBT is continuously decreasing, and the 6 IGBTs exhibit a slightly lower temperature on both sides and a slightly higher intermediate temperature, which is determined by the relative

position of the IGBT arrangement and the water channel. The steady-state temperature at 4 L/min was 55.25 °C.

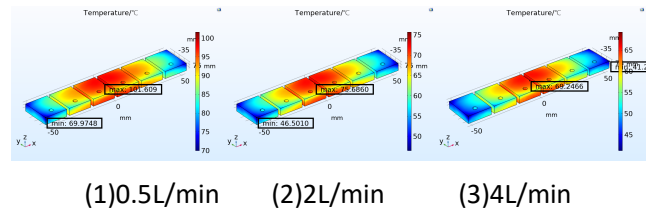


Fig. 7 IGBTs temperature rise distribution under different flow rates

## 4. EXPERIMENTAL RESULTS AND DISCUSSION

### 4.1 Experiment platform

Fig. 8 shows the experimental platform connection principle block diagram, which mainly composed of the following parts in Table 3.

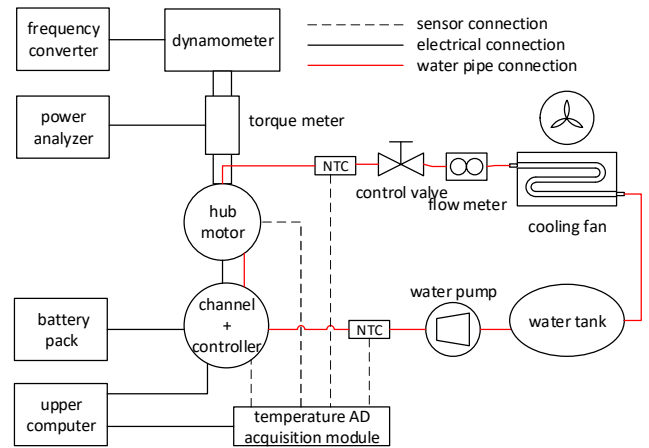


Fig. 8 Experimental device connection schematic

Table 3. Experimental bench composition

System	Contents
Test system	dynamometer, frequency converter, torque meter-JN-338, power analyzer-JN-338
Cooling system	water pump-2440T, flow meter-K24, control valve, water tank, cooling fan
Motor system	in-wheel motor, external water channel, controller, battery pack-200V
Accessories	upper computer, temperature ATD acquisition module

## 4.2 Experimental results

Fig. 9 shows the temperature rise of the stator winding under different flow rates. It can be seen that except for the individual error conditions, the measurement of the 9-channel temperature sensor is basically the same.

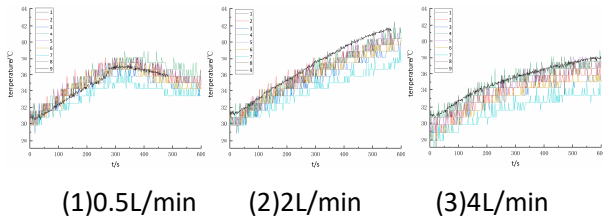


Fig. 9 Temperature rise curves of stator windings under different flow rates

Fig. 10 shows the temperature rise under different flow rates. It can be seen that when the motor reaches the operating point, the IGBT temperature will rise rapidly, and then the cooling will continue due to the continuous circulation of the cooling water. It has been reduced and kept stable. It can be found that the temperature of the IGBTs in the middle is higher than the others, which is quite consistent with the simulation results, which verifies the correctness of the simulation results.

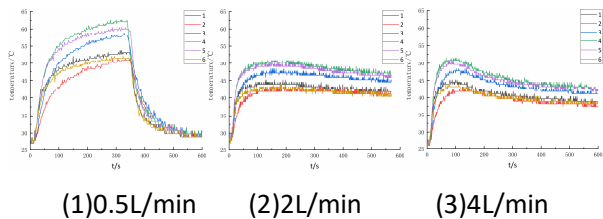


Fig. 10 Temperature rise curves of IGBTs under different flow rates

## 4.3 Discussion

Table 4 shows the statistics of the original thermal problem, and the following points can be summarized.

1. The initial temperature rise of the IGBT is very fast, up to 60 °C, and then the temperature drops back. Due to the installation position, the six discrete IGBTs have a high intermediate temperature and a low edge temperature, which is consistent with the finite element simulation results. Compared with the waterless channel, the temperature rise after cooling decreases by 49.65 °C.

2. The temperature variation of the winding is obvious, and gradually transitions along the circumferential direction. As the cooling flow increases, the overall temperature rise gradually decreases. Similarly, the

temperature rise drops by 31 °C compared to the no heat dissipation state.

3. 4 L/min under the water channel is the optimal cooling flow, and the cooling effect on the motor is better.

Table 4. No cooling, FEM and experimental results

Type	No cooling	FEM	Experimental value	Simulation error
IGBT	100.22	55.25	50.57	9.2%
Winding	69.27	35.8	38.2	6.3%

## 5. CONCLUSIONS

This paper studies the heat dissipation characteristics of the integrated controller in-wheel motor. On the basis of the serious motor heating problem, the double-sided combined water channel is used to achieve simultaneous cooling of the motor stator and controller. The experimental results show that the motor has good heat dissipation effect and the temperature rise of the winding is reduced to 38.2 °C, the IGBT is reduced to 50.57 °C, the optimal cooling water flow is determined to be 4 L/min. The finite element simulation error is less than 6.3 %, indicating that the model has high precision.

## ACKNOWLEDGEMENT

The authors greatly appreciate the financial help from Low Emission Vehicle Research Laboratory(LEVRL).

## REFERENCE

- [1] Nollau A, Gerling D. A new cooling approach for traction motors in hybrid drives. Proceedings of the 2013 IEEE International Electric Machines and Drives Conference: 2013 IEEE International Electric Machines and Drives Conference, 2013:456-461.
- [2] Luise F, Tassarolo A, Agnolet F, et al. A high-performance 640-kW 10.000-rpm Halbach-array PM slotless motor with active magnetic bearings. Part I: Preliminary and detailed design. 2014 International Symposium on Power Electronics, Electrical Drives, Automation and Motion, 2014:1237-1244.
- [3] Xiaoyi Li, Zhiguo Tang, Danyang Zhao, et al. Analysis of heat dissipation characteristics of double channel liquid cooled permanent magnet synchronous motor. Journal of Hefei University of Technology(Natural Science) 2018;41(6):726-730.